A Change in Twist of Actin Provides the Force for the Extension of the Acrosomal Process in *Limulus* Sperm: the False-discharge Reaction

DAVID J. DEROSIER, LEWIS G. TILNEY, EDWARD M. BONDER, and PHYLLIS FRANKL
Rosenstiel Basic Medical Sciences Research Center, Brandeis University, Waltham, Massachusetts 02254; and the Department of Biology, University of Pennsylvania, Philadelphia, Pennsylvania 19104

ABSTRACT One of the most spectacular motions is the generation of the acrosomal process in the *Limulus* sperm. On contact with the egg, the sperm generates a 60-μm-long process that literally drills its way through the jelly surrounding the egg. This irreversible reaction takes only a few seconds. We suggested earlier that this motion is driven by a change in twist of the actin filaments comprising the acrosomal process. In this paper we analyze the so-called false discharge, a reversible reaction, in which the acrosomal filament bundle extends laterally from the base of the sperm and not anteriorly from the apex. Unlike the true discharge, which is straight, the false discharge is helical. Before extension, the filament bundle is coiled about the base of the sperm. In the coil, the bundle is not smoothly bent but consists of arms (straight segments) and elbows (corners) so that the coil looks like a 14-sided polygon. The extension of the false discharge works as follows: Starting at the basal end of the bundle, the filaments change their twist which concomitantly changes the orientations of the elbows relative to each other; that is, in the coil, the elbows all lie in a common plane, but, after the change in twist, the plane of each elbow is rotated to be perpendicular to that of its neighbors. This change transforms the bundle from a compact coil into an extended left-handed helix. Because the basal end of the bundle is unconstrained, the extension is lateral. The true discharge works the same way but starts at the apical end of the bundle. The apical end, however, is constrained by its passage through the nuclear canal, which directs the extension anteriorly. Unlike the false discharge, during the true discharge the elbows are melted out, making the reaction irreversible. This study shows that rapid movement can be generated by actin without myosin and gives us insight into the molecular mechanism.

Albeit motility is a common feature of the cytoplasm of all eucaryotic cells, in most cases the mechanism or mechanisms for that motion are either not understood at all or incompletely understood. The two best-studied systems are skeletal muscle contraction and flagellar movement. Since both of these have as their bases a sliding of units relative to each other, under the direction of an ATPase, (i.e. myosin or dynein) many investigators have tried to explain other motile events in cells in similar terms, particularly since most (if not all) eucaryotic cells contain a great deal of actin and tubulin. In certain cases such as cytokinesis and clot retraction this has met with some success, but in others it appears that such a unified hypothesis does not apply and it is necessary to think of different mechanisms such as the assembly of the polymer, formation or disassembly of a gel, bundle formation, or even the interaction of actin or tubulin with other kinds of filaments. The major difficulty in obtaining information on many of these systems is that they are quite disordered and one cannot easily isolate the motile cytoplasmic region in working condition. In fact, even to identify the structural units and their interactions is exceedingly difficult because the structures are labile to isolation methods, fixation, etc. An exception to this is the bundle of actin filaments that gives rise to the acrosomal process in *Limulus* sperm. This bundle is of interest as a model system: the bundle is highly ordered and therefore amenable to structural studies; it can be isolated and characterized chemically; and the generation of this process appears to be driven by an entirely novel mechanism involving a change in twist of the

THE JOURNAL OF CELL BIOLOGY · VOLUME 93 MAY 1982 324-337

actin-containing filaments (5). No myosin seems to be needed.

The generation of the process is spectacular. Association of the sperm with the egg triggers the opening of the acrosomal vacuole which is followed immediately by the explosive discharge of a long, generally straight structure, the acrosomal process (1). The full 60-μm length that emerges from the anterior end of the sperm is discharged in only 5 s, but what is particularly striking is the rotation of the extending structure, which gives the impression that it is drilling its way through the jelly layers surrounding the cytoplasmic membrane of the egg (10).

A second, and somewhat curious reaction in this sperm, is the so-called false discharge (1) in which a sinusoidal structure is generated from the posterior end of sperm. This reversible reaction, which has no known physiological role, is even faster than the true discharge. Both the true and the false discharges involve the uncoiling of a preformed bundle of filaments present within the unreacted sperm, the former starting at the apical end of the bundle and the latter at the distal end.

The filament bundle in the true discharge has the appearance of an actin paracrystal: it consists of a parallel array of actin filaments in which the crossover points of adjacent actin helices are in almost perfect register. The spacing between filaments (85 Å) in the bundle is substantially larger, however, than that observed in pure actin paracrystals (~60 Å). Three-dimensional reconstruction of the bundle generated from electron micrographs shows that the filaments have the appearance of actin that has been coated on its outer edge by additional material (3). This additional material presumably corresponds to one or both of the proteins found with actin in the bundle (10). One of these proteins, scruin, has a molecular weight of 55,000 and is present in equimolar proportions with actin. The second protein has a molecular weight of 95,000 but is present in one-fourth the amount of actin.

In an earlier publication (5) we described the changes involved in the extension of the true discharge. We suggested that it is a change in twist of the actin filaments that drives this extraordinary motion. In this paper we describe the changes involved in the extension of the false discharge, and relate these changes to those of the true discharge. We conclude that extension of both the true discharge and the false discharge is accounted for by the same mechanism and, in fact, is closely related. In short, both motions can be explained by a change in the twist of the actin-containing filaments. This study, then, reinforces and extends our earlier publication showing how rapid movement can be generated with actin without myosin and tells us more about the molecular mechanism of this motion.

MATERIALS AND METHODS

Obtaining Sperm

Limulus polyphemus were collected by the supply department of the Marine Biological Laboratory, Woods Hole, MA and kept in tanks with running sea water. *Limulus* were also maintained in 100-gal aquaria at the University of Pennsylvania and Washington University Medical School (St. Louis, MO) in artificial sea water (Instant Ocean, Aquarium Systems, Mentor, OH). When sperm were needed the organism was milked (see reference 10) and the spermatozoa were collected by centrifugation (5,000 *g* for 5 min).

Observation of Living Sperm

Limulus sperm were examined with a Zeiss phase microscope with oil immersion optics. Photographs were taken with a Leitz microipso attachment; movies were taken with a 16-mm Bolex camera attached to the microscope with a homemade stand.

Isolation of the False Discharge, True Discharge, and Coil

THE FALSE DISCHARGE: A pellet of *Limulus* sperm was extracted with 1% Triton X-100, 3 mM $MgCl_2$ and 30 mM Tris HCl at pH 8.0. This induces the sperm to form the false-discharge form of the filament bundle. The suspension was then centrifuged at 2,500 *g* for 5 min to remove the chromatin, and the supernate which contained false discharges and flagellar axonemes was centrifuged at 10,000 *g* for 10 min which pelleted both those elements. To purify the false discharges further, it was necessary to solubilize the flagellar axonemes which can easily be done by incubating the pellet in 0.5% sarkosyl in 10 mM Tris HCl at pH 7.5 for 15 min at 0°C. The clean pellet of false discharges then could be had by centrifugation.

THE TRUE DISCHARGE: Sperm were suspended in sea water containing 50 mM $CaCl_2$, and then an ionophore, A23187 (Calbiochem-Behring Corp., San Diego, CA), was added. A stock solution containing 1 mg/ml A23187 dissolved in dimethylsulfoxide was made, and for each milliliter of sperm solution 15 μl of this stock was used. The stock was kept in the dark and refrigerated when not being used. The ionophore induced the acrosomal reaction within 1 min, but beginning at that time the DNA in the nucleus becomes uncoiled forming a gel. Thus, to isolate the true discharge one must digest away the DNA by DNase 1. For Fig. 2 we used an undigested sample so that there is DNA around this bundle.

THE COIL: Although there are several ways of obtaining coils, for this paper we fixed the sperm briefly (1 min) in 1% glutaraldehyde (Electron Microscope Sciences, Fort Washington, PA) in sea water and then added the suspension to a large volume of 1% Triton X-100, 3 mM $MgCl_2$ and 30 mM Tris at pH 8.0. The brief fixation inhibits the formation of a false discharge. The membranes are solubilized and the coil falls away from the nucleus.

NEGATIVE STAINING: Isolated false discharges were washed and then a drop was placed upon a colloidin-coated grid that was stabilized by a thin layer of carbon. Negative staining was carried out using a solution of 1% uranyl acetate.

REPLICAS: The false discharge or sperm were fixed, extracted with Triton X-100, placed upon a freshly cleaved surface of mica, and air dried. The mica was then placed in a vacuum evaporator and rotary shadowed with platinum followed by carbon. The replica was then floated off onto a solution of the laundry bleach, Clorox, where the biological part was digested away. The replica was then washed, picked up on grids, and examined with a Philips 200 electron microscope.

FAST FREEZING, FREEZE ETCHING, AND ROTARY SHADOWING: The specimens illustrated in Fig. 2 were prepared as follows. A pellet of the isolated bundles was placed on a thin slice of fixed and washed lung and rapidly frozen by dropping the sample onto a block of copper cooled to liquid helium temperatures (6). The frozen pellet was then freeze fractured on a Balzars 200 apparatus at −170°C (Balzars, Hudson, NH), etched for 5 min at −92°C, and rotary shadowed with platinum followed by carbon. The replica, after digestion in chromic acid and washing, was examined in a JEOL 100 electron microscope.

ANALYSIS OF ELECTRON MICROGRAPHS: Optical diffraction patterns were recorded directly from the electron microscope plates on the optical diffractometer described by Salmon and DeRosier (8).

Computed diffraction patterns were obtained as follows. Micrographs were scanned on an Optronics P1000 (Optronics International Inc., Chelmsford, MA) using a 50-μm raster. Fourier transforms were computed on a PDP 11/40 according to DeRosier and Moore (4), and the squared amplitudes were displayed on a Grinnell gray-scale, graphics terminal (Grinnell Systems Corp., Santa Clara, CA). Measurements of layer line spacings were made using a centroid locating program kindly made available to us by Ed Egelman (Graduate Program in Biophysics, Brandeis University). For display, the computed patterns are photographed directly from the Grinnell video monitor.

COMPUTER SIMULATION OF THE FALSE DISCHARGE: To animate the false discharge, the motion of each elbow was divided into 30 three-degree rotational increments. For each increment, the form of the bundle is calculated on a PDP 11/40 computer (Digital Equipment Corp., Maynard, MA). These values are then stored on disk. 300 frames are stored and then rapidly run through the graphics terminal to produce the animation. The figures displayed in Fig. 11 were obtained by redirecting six frames of data from the animation program through a plotting program to a Tektronix pen plotter (Tektronix, Inc., Beaverton, OR).

RESULTS

The Structure and Antics of Limulus Sperm

Unreacted *Limulus* sperm have an amazingly complex morphology. To understand what happens to the actin filament

bundle in the generation of the false discharge it is essential for the reader to recall some of this complexity. Accordingly, we are including in this subheading a brief summary aided by drawings of the basic morphology of *Limulus* sperm to help those readers not familiar with its complexity. Further details can be found in André (1), Tilney (10), DeRosier et al. (3, 5), and Tilney et al. (11). The new information included in this report begins under the next subheading.

In unreacted *Limulus* sperm (Fig. 1 *b*), there is a bundle of actin-containing filaments that extends from the basal end of the acrosomal vesicle through a channel in the nucleus; this channel is lined by both the outer and inner nuclear membranes. At the base of the nucleus the inner nuclear membrane fuses with the inner membrane covering the base of the nucleus, thus creating a toroidal inner nuclear membrane. The filament bundle in this region, still sheathed by the outer nuclear membrane, continues down to the basal body of the flagellum, where it moves to the lateral margin of the cell and is coiled in a space between the basal portions of the outer and inner nuclear envelopes. In the coil it remains sheathed by the apical surface of the outer nuclear membrane and therefore is topologically in the cytoplasm. The most posterior end of the bundle can extend from the coil posteriorly as the false discharge (Fig. 1 *a*). The anterior end can extend anteriorly and in reacted sperm will be situated at the tip of the acrosomal process (Fig. 1 *c*). This latter is the true discharge.

Careful examination of the coil either by negative staining, thin sectioning, or freeze fracturing and rotary shadowing reveals that it is not smoothly bent but rather has corners so that each loop of the bundle takes on a polygonal form with 14 straight segments (arms) and 14 corners (elbows) (Fig. 2 *b*). Each arm has a length of 0.7-μm, and the elbows make an angle of 156°. A freeze-etched, rotary-shadowed preparation of coils shows that the filaments wind around the bundle with a right-handed sense, making one turn every 4.2 μm (see reference 5). In contrast to the coil, the true discharge does not have elbows, nor is it supercoiled (Fig. 2 *c*). Thus, in going from the coil to the true discharge the bundle has lost its elbows and changed its supercoiling by 360° per 4.2 μm discharged. The latter change gives rise to the drilling motion seen in movies of the true-discharge reaction: that is, as the bundle extends 4.2 μm outwards, the change in supercoiling produces a rotation of the bundle by 360°, a value we can experimentally measure from movies of reacting sperm. What is important is that in going from the coil to the true discharge the change in supercoiling is correlated with a change in twist of the actin filaments themselves: that is, each actin filament untwists by an amount exactly equal to the amount of supercoiling. From this and other data we suggested in our last report (5) that a change in the twist of the actin filaments themselves generates motion. What follows here is an analysis of the false discharge similar to that carried out for the true discharge (5). In the Discussion, then, we will examine the relationship between these three stable forms of the filament bundle and discover how one form changes into another.

During Generation of the False Discharge the Bundle Rotates

When sperm are diluted into sea water or when the tonicity of the sea water is increased, the false discharge, with its characteristic 2.8 μm sinusoidal shape appears (Fig. 1 *a*). If these sperm are induced to undergo the acrosomal reaction either by high calcium or high calcium and an ionophore such as A23187 or X537A, the false discharge is first retracted, then the true discharge appears. Alternatively, if the detergent, Triton X-100, is perfused past the sperm, the filament bundle in the coil is rapidly converted into the false discharge. The speed of elongation and the length of the false discharge depend on the treatment. If the sperm are perfused with Triton, the entire coil is transformed into the false discharge. This occurs in ~1 s. If the false discharge is induced with milder treatment (i.e. hypertonic sea water or dilution), only a portion appears. The speed of elongation is variable and can occur over many seconds. Movies of these events were taken and analyzed frame by frame. One sequence is shown in Fig. 3 *b*. Careful analysis of the movies proves that the bundle is indeed helical and as it extends it rotates, tracing out a left-handed helix. To illustrate this we have drawn cartoons (Fig. 3 *d, e, f*) showing the expected behavior of the bundle depending on its structure and whether or not it rotates during extension.

In Fig. 3 *d* we show the expected sequence if the bundle is helical and screws its way outward. It is necessary to examine the sequence carefully and to compare it with that in 3 *e* and 3 *f*. In 3 *d*, the bundle at its entry into the body of the sperm is at a trough of the wave and it remains so as the bundle extends. The advancing tip, on the other hand, begins (top of 3 *d*) at the crest of a wave and in succeeding sequences moves down into

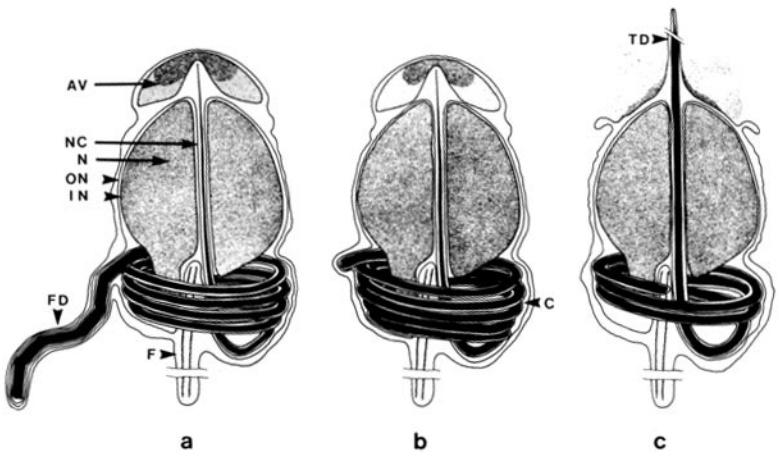

FIGURE 1 Schematic view of the actin filament bundle in the sperm of *Limulus*. (*a*) The false discharge. If the sperm is exposed to hypertonic sea water or is extracted with a 1% solution of Triton X-100, a false discharge is generated. The discharge begins at the basal end of the bundle and extends outward laterally. In the figure a short segment of false discharge is shown. (*b*) The unreacted sperm. In the unreacted sperm the bundle is coiled. It begins under the acrosomal vesicle, proceeds through the nucleus, and is coiled about the base of the sperm between the inner and outer nuclear membranes. The bundle, by carrying with it the anterior nuclear membrane, remains a cytoplasmic structure. (*c*) The true discharge. When the sperm is treated with the ionophore A23187, it undergoes the true discharge reaction. The reaction begins with the opening of the acrosomal vesicle and is followed immediately by a complete uncoiling of the bundle which generates the 60 μm-long acrosomal process. Abbreviations: *N*, nucleus; *F*, flagellum; *AV*, acrosomal vesicle; *C*, coil; *FD*, false discharge; *TD*, true discharge; *NC*, nuclear canal; *ON*, outer nuclear membrane; *IN*, inner nuclear membrane.

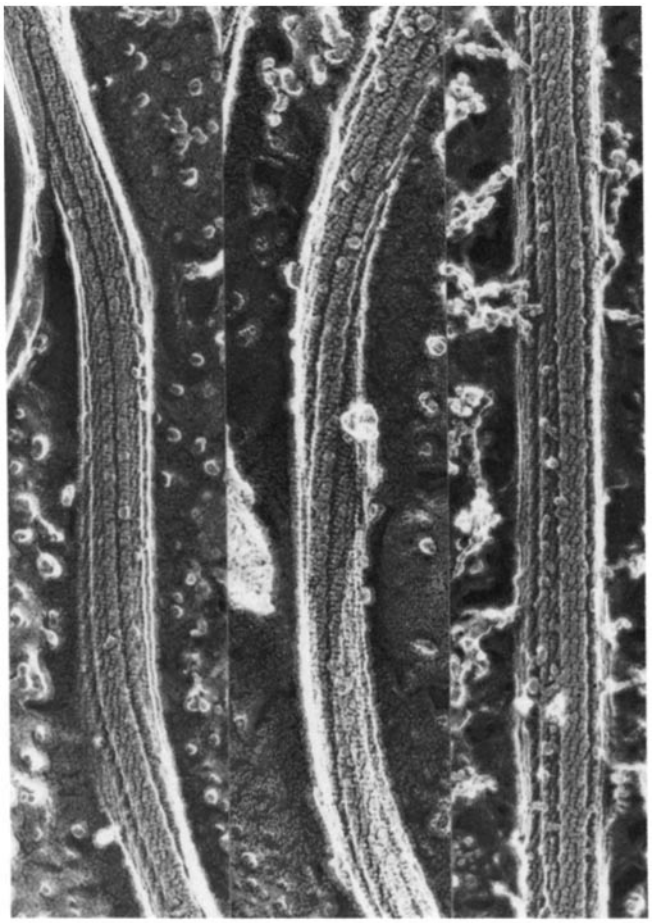

FIGURE 2 Electron micrograph of the frozen, etched bundle. (*a*) The false discharge. The arms and elbows are easily seen as is the supercoiling. The rows of filaments generate edges which can be seen to start at the lower right edge of the bundle and move to the upper left. This establishes the supercoiling as left-handed. (*b*) The coil. As in (*a*), the arms and elbows are easily seen. Note that the supercoiling is right-handed, that is, the filaments start at the lower left of the bundle and cross to the upper right. Note also that the amount or rate of supercoiling is greater here than in the false discharge. (*c*) The true discharge. The arms, elbows and supercoiling are absent. × 100,000.

a trough and then back up to a crest (see bottom of Fig. 3*d*). Thus, if the filament is a helix that screws its way outward the tip will appear to undulate, tracing out the path of the wave, while the crests and troughs of the waves appear stationary.

In Fig. 3*e* we illustrate the behavior expected if the bundle is either helical or a planar sine wave and is pushed out without any rotation. The differences between 3*d* and 3*e* are subtle. Note first that the bundle at its juncture with the body of the sperm is at a trough. As elongation proceeds, however, it shifts. Midway down in 3*e*, it is at a crest and, then, at the bottom again at a trough. The advancing tip of the wave, unlike the case in 3*d*, does *not* trace out the path of the wave. It begins at the tip of a crest and remains there as elongation proceeds. Thus, if there is no rotation, the crests and troughs move outward with elongation while the advancing tip remains at the crest of the wave. This is the opposite to the behavior in 3*d*.

In 3*f* we show the behavior if the false discharge has a planar sinusoidal form and rotates. As it rotates by 90° so that we look along the plane of the wave, the crests and troughs disappear (see middle of 3*f*). When it rotates by 180°, the crests and troughs reappear.

Looking back now at the movie frames in Fig. 3*b*, we see that the motion corresponds to 3*d*. In the first frame the advancing tip is at the crest of a wave. In frame 3 it is at the trough and in frame 6 it is again at a crest. Furthermore, if we examine the positions of the crests and troughs we see that they appear fixed during extension. Thus, the bundle screws its way out, turning through 360° with every 2.8 μm (1 repeat) of extension.

The Bundle in the False Discharge Consists of Arms and Elbows

When the false discharge is examined either by negative staining or in a replica it is clear that, although the bundle takes the form of a helix, it is not a smooth helix, but the helix consists of arms and elbows which are similar to those in the coil. To better compare the arms and elbows in the two forms, we have measured the lengths of the arms and the angles of the elbows (see Table 1). In both the coil and the false discharge, the arms are 0.7 μm in length and the elbows make an angle of 156°. In the false discharge the helical repeat occurs approximately every 2.8 μm and consists of four arms and four elbows as is evident in Fig. 4. Keep in mind that in the negatively stained image the bundle is flattened and its form appears to be planar rather than helical. The helical nature of the bundle can be best appreciated in replicas.

The Bundle in the False Discharge is a Left-handed Filamentous Helix

To determine the hand of the false-discharge helix, we examined freeze-etched replicas of the purified false discharges. Although images that clearly show the hand were difficult to find, we did find a few. One of these is shown in Fig. 5, together with a sketch of a left-handed helix. The image shows a piece from the bottom of the helix, the top half being cleaved off. In the image the lower end is seen to be curving up toward the right hand of the reader while the top is coming up and to the left. This can only be from a left-handed helix. Although only a few examples have been found we believe, on the basis of measurements of superhelicity of the filaments, that all the bundles necessarily have the form of a left-handed helix.

The Filaments in the False Discharge are Supercoiled with a Left-handed Sense

By examining freeze-etched bundles after the false discharge, we find that the filaments coil about the bundle axis with a left-handed sense. This can be easily seen in Fig. 2*a*. In the figure, a filament that has just come into view at the lower right-hand edge, will eventually disappear off the upper left-hand edge. The helix described by this filament is left handed. We have examined several dozen micrographs and found in all cases that the filaments are supercoiled with a left-handed sense.

In the False Discharge the Amount of Supercoiling of the Filaments is 30° Per Arm

The amount of supercoiling can be deduced from the repeat of the Moiré patterns seen in each arm. This procedure was

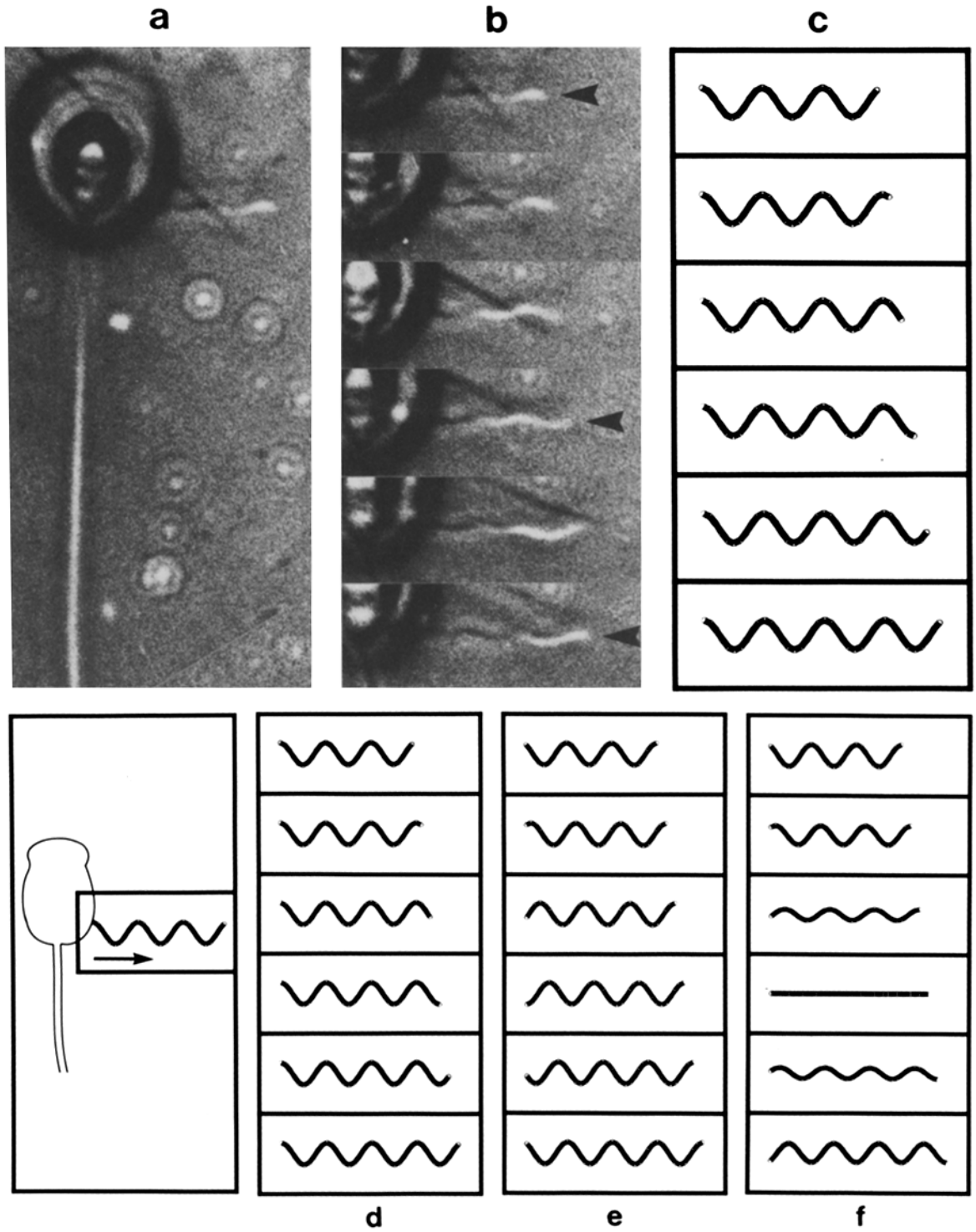

FIGURE 3 The false-discharge reaction. (*a*, *b*) Prints from selected frames of a movie taken during a false discharge. In (*a*) the whole sperm is shown with the false discharge extending laterally to the right. In (*b*) the sequence is shown for the discharge of one repeat or 2.8 μm. Frames correspond to intervals of 160 ms. (*c*) Drawing of the bundle in (*b*). What is important to note is the advancing end of the bundle. In the top frame, the advancing tip of the bundle is at the crest of a wave (see arrow). As we move to the middle frames we see that this tip has slid down the crest and lies in a trough (see arrow). In the last two frames it climbs again to return to the crest of the wave (see arrow). (*d*, *e*, *f*) Schematic drawings of three possible modes of extension. In (*d*) the bundle is helical and is screwing its way outward. Note that the advancing tip starts at the crest of a wave, slides down to a trough, and climbs again to a crest. This is exactly the motion seen in (*b*). In (*e*), the bundle is helical or a planar sine wave but is just being pushed without rotation. Note that the advancing tip starts on the crest of a wave and remains so in the rest of the frames. The motion is clearly different from the movie frames shown in (*b*). In (*f*) the bundle is planar sine wave and is rotating as it extends. Note that when the bundle rotates through 90° we see it edge on and it appears straight (see middle frame in *f*). As the bundle rotates further, the crests and troughs appear to interchange. This is not seen in the movie. × 3,600.

TABLE I

Determination of Arm Length and Elbow Angle in the Coil and in the False Discharge

Structure	Arm length	Elbow angles
	A	*Degrees*
Coil	6,800 ± 300 (n = 23)	156.0 ± 0.6 (n = 31)
False discharge	7,200 ± 300 (n = 59)	156.6 ± 0.5 (n = 100)

initially applied to the coil (see reference 5) and works as follows:

In the false discharge, the true discharge, or the coil, the filaments are hexagonally packed (see reference 10). Examine the drawing of the supercoiled bundle of seven hexagonally packed filaments shown in Fig. 4*a*. At the left-hand edge of the bundle the filaments are directly over each other, i.e. filament *B* is directly above *A*, *C* directly above *O* and *F*, and

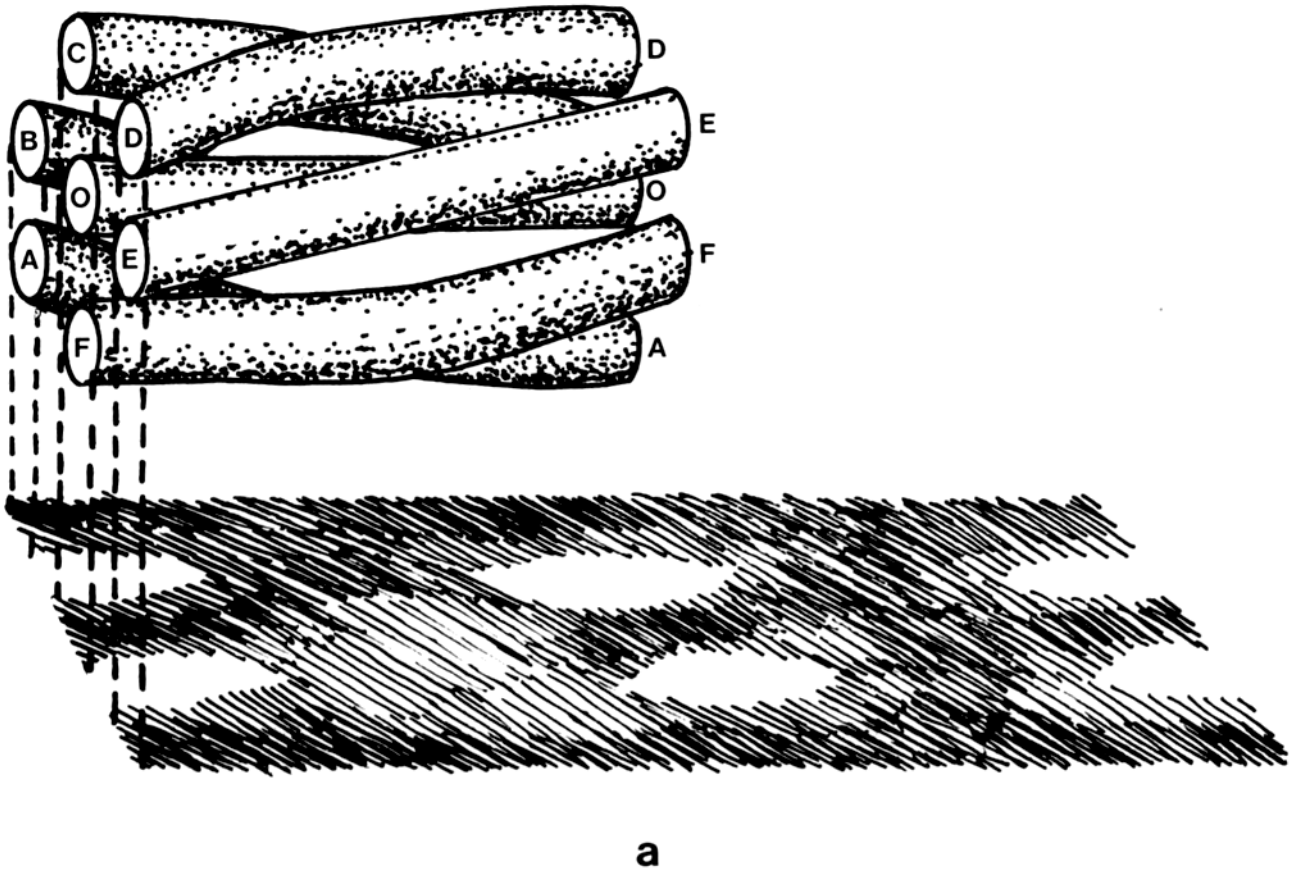

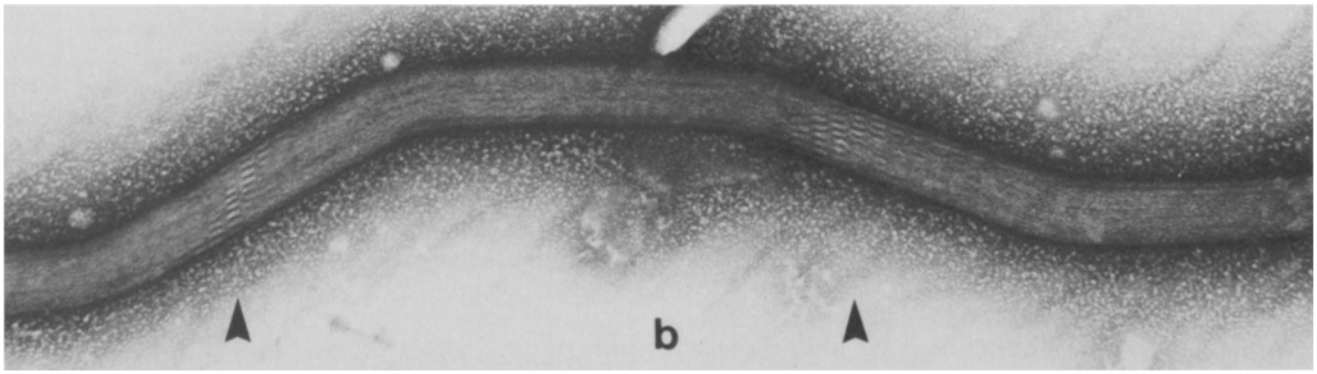

FIGURE 4 Moiré patterns in the supercoiled bundle. (*a*) Schematic diagram showing how the Moiré pattern arises. Shown in the figure is part of a supercoiled bundle and its shadow. At the left-hand end of the shadow we see three stripes separated by two gaps. The foremost stripe corresponds to the shadow of filaments *D* and *E*, the central stripe of the shadow to *C*, *O*, and *F*, and the rearmost stripe to *A* and *B*. As we move along the shadow to the right, we lose the gaps and have a solid shadow. This happens because the bundle is supercoiled and the filaments no longer lie over one another. When the bundle has undergone 60° of supercoiling the filaments again superpose but this time *E* and *F* give rise to the foremost stripe, *D*, *O*, and *A* to the central stripe, and *C* and *B* to the rearmost stripe. Thus, the amount of supercoiling in a repeat of the shadow is 60°. The shadow, but not the bundle, has been extended one more repeat. (*b*) Electron micrograph of a negatively stained image of the false discharge. The patches where filament superposition occurs are marked with arrows. The pattern repeats every other arm. Thus, the amount of supercoiling is 30° per arm. × 71,000.

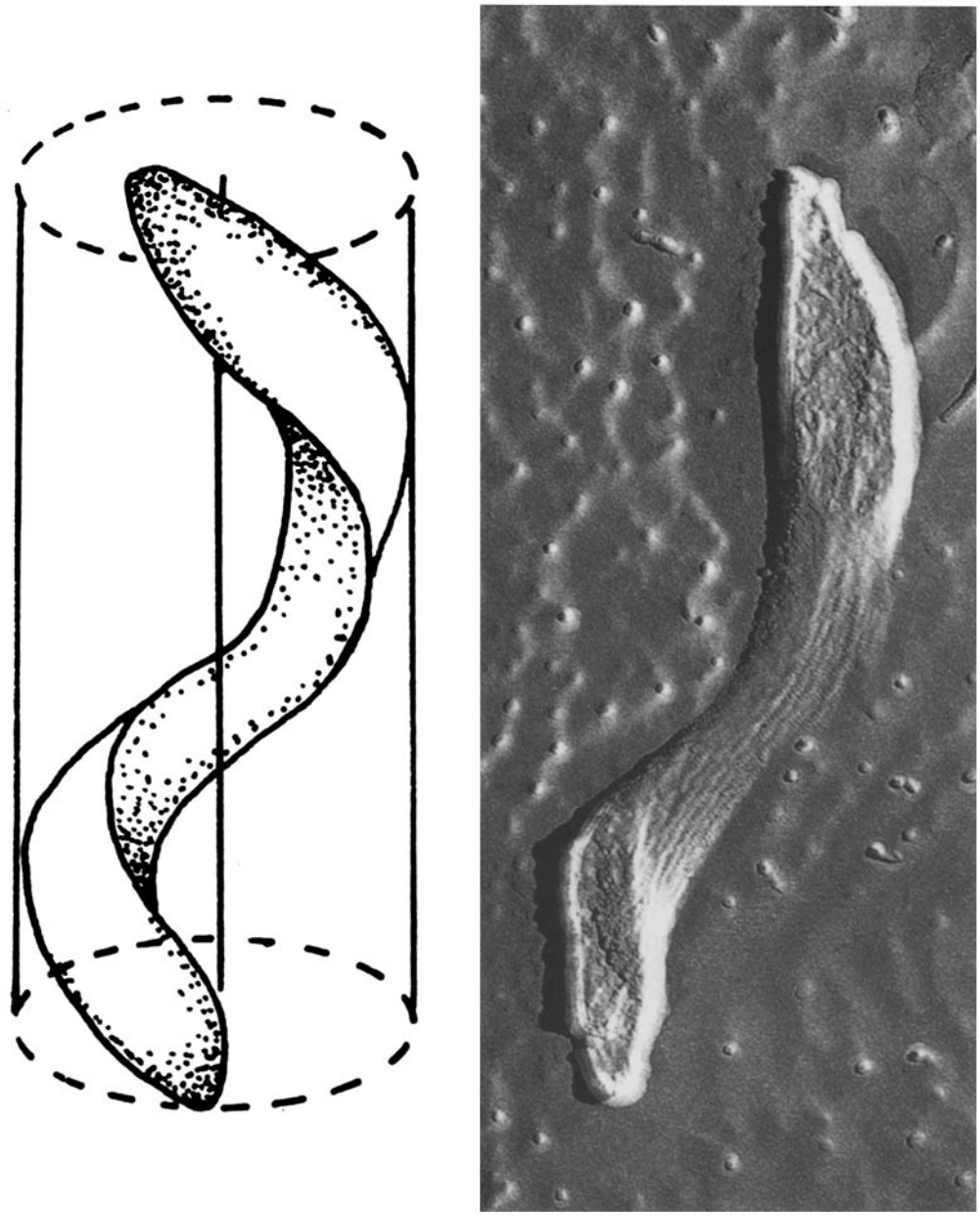

FIGURE 5 Freeze fracture of the false discharge. The figure shows that the bundle is left handed. To aid the reader, a sketch of a left-handed bundle is included. × 175,000.

D directly above *E*. If we imagine an overhead light source and look at the shadow or projection, we will see three shadows separated by two gaps (see left-hand edge of shadow), the backmost shadow being due to filaments *A* and *B*, the central shadow being due to *C*, *O*, and *F*, and the foremost shadow arising from *D* and *E*.

Since the bundle is supercoiled, the relationships between the filaments change as we move along the bundle. Halfway down the bundle, we see that filaments *F* and *D* have moved so that their shadows fill in the foremost gap while *C* and *A* similarly have cast shadows in the backmost gap. As a result the corresponding segment in the shadow shows no gaps. After 60° of supercoiling, however, we again get superposition of filaments. This time filament *E* is above *F*, *D* above *O* and *A*, and *C* is over *B*. In the shadow, we again see three strips and two gaps. The shadow but not the bundle is extended one more repeat to show more clearly the pattern of gaps. The important point is that each repeat of the pattern corresponds to 60° of supercoiling.

Let us now apply this to the electron micrographs of the false discharge. There are two regions where the filaments are clearly seen (see arrows in Fig. 4*b*). These are separated by an arm which has no clear view of the filaments. Thus, in a space of two arms the bundle has undergone 60° of supercoiling or 30° per arm with a left-handed sense as determined from the freeze-etched specimens. In contrast, the filaments in the coil, the precursor to the false discharge, are supercoiled to the right and by 60° per arm.

The Twist of the Actin Filaments in the False Discharge is Different from That in the Coil

The twist of the actin filaments and the amount and hand of supercoiling are coupled (5); that is, for every degree of change in supercoiling there must necessarily be a corresponding degree of change in the twist of actin, and these changes must agree in hand or direction as well as in amount. In going from the coil to the true discharge, the supercoiling changes by 60° per 0.7-μm arm. In one arm there are 260 actin subunits; thus, each subunit should be twisted by $-60°/260 = -0.23°$, the

minus sign indicating a left-handed sense. From the diffraction patterns of the coil and true discharge, DeRosier et al. (5) measured $-0.23° \pm 0.05°$.

In going from the coil to the false discharge, the change in supercoiling is 90° per arm in a left-handed sense and therefore the expected change in twist is $-90°/260 = -0.35°$ per subunit. From five segments of the false discharge we computed diffraction patterns (Fig. 6*b*) and, using equation 1 in DeRosier et al. (5), we determined a value of $-0.34° \pm 0.06°$ which agrees in hand and amount with the prediction based on the change in supercoiling.

Kinks in the True Discharge are Segments Having the False-Discharge Configuration

Sperm were placed on a slide, examined with a microscope, and then perfused with sea water containing 50 mM $CaCl_2$, a treatment that induces some of them to form the true discharge, and then perfused with a solution containing 1% Triton X-100. On several occasions sperm that were in the process of undergoing the true discharge were simultaneously induced by the Triton solution to also form the false discharge. The end result is that the filament bundle, which is continuous through the nucleus, has the true discharge extending from the base of the nucleus anteriorly continuous with the false discharge which extends from the nucleus posteriorly. Thus, the true- and false-discharge segments can exist in the same filament bundle. In this case the true discharge is at one end and the false discharge at the other.

Often during the true discharge we see kinks in the otherwise straight bundle. What is more important is that segments having the false-discharge configuration can occur within regions of true discharge. These kinks, which aid us in determining the amount of rotation of the true discharge (5), are actually stretches of helix having a 2.8-μm repeat, the repeat of the false discharge. In fact, these kinks are indeed segments of the same helix seen in the false discharge: the kinks have a repeat of 2.8 μm (see Fig. 7*a* and *b*) and in the electron microscope consist of arms and elbows (Fig. 7*c*). As would be expected for a false discharge, each kink has four arms and four elbows. Thus, segments of the false-discharge helix are normally found in the true discharge, although they appear at random in the true discharge.

The False Discharge Transforms into the True Discharge In Vitro

If a preparation of false discharges is not used immediately, an increasing number "straighten out": that is, they no longer present their characteristic undulatory profile. Although this has not been adequately worked out, some preparations of the false discharge can be converted to the true discharge in minutes. Examination of these straightened false discharges by negative staining or in replicas shows that they are indeed true discharges with no supercoiling of the filament bundles (see Fig. 8). Often these treated bundles show residual regions of the false-discharge helix separated by straight segments characteristic of the true discharge.

Handedness of the Coil

Although the supercoiling, the hand, and the twist of the filaments in the coil were covered in our last paper (5), we have subsequently established the handedness of the coil proper. We wish to know whether all coils are left handed, whether all are right handed, or whether some are right handed and some are left handed.

Sperm were fixed briefly (1 min) in glutaraldehyde in sea water and then detergent extracted. This brief fixation inhibits the formation of the false discharge when the sperm are detergent extracted. The sperm were then dried on a piece of freshly cleaved mica and rotary shadowed with platinum. The replica was floated off, the sperm digested away, and the replica placed on grids. Great care was taken not to inadvertently flip the replica which would cause us to incorrectly determine the

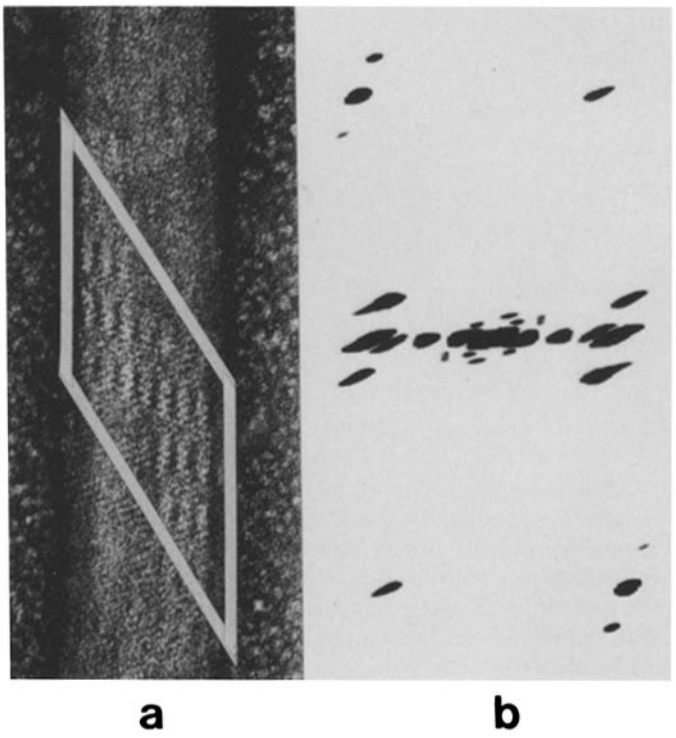

FIGURE 6 Determination of the twist of the filaments. (*a*) Electron micrograph of a negatively stained false discharge. The box shows the region of the particle we used to calculate the diffraction pattern. × 215,000. (*b*) Computed diffraction pattern. The region marked in (*a*) was digitized and the diffraction pattern calculated. From the spacings of the layer lines, the symmetry or twist of the actin filaments was computed. The first and the sixth layer lines are indicated.

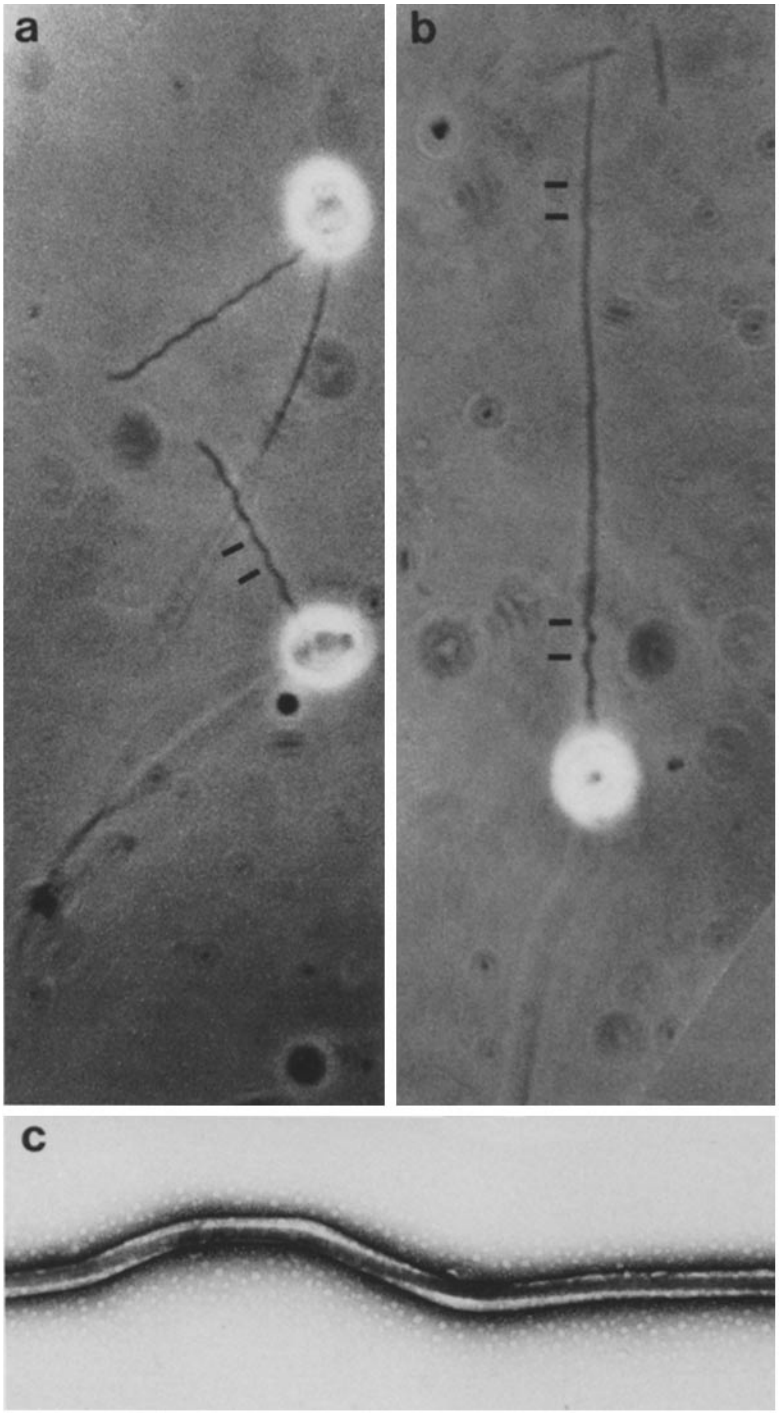

FIGURE 7 Kinks seen in the true discharge. (*a*) The false discharge. The false discharge is shown as seen in the light microscope for comparison. The 2.8 μm repeat is marked with bars. (*b*) The true discharge showing kinks. The period of the kinks is marked and is clearly the same as that of the false discharge. × 1,600. (*c*) Electron micrograph of a negatively stained kink. In the micrograph the kink can clearly be seen to be composed of four arms of length 0.7 μm and four elbows. It has the same structure as the false discharge. × 21,000.

hand. Upon drying, the coil falls away from the nucleus and lies on the grid with the anterior side upwards, or that side formerly in contact with the nucleus (Fig. 9). As shown by Tilney (10) and Tilney et al. (11), the filament bundle, after it exits from the nuclear canal, coils up below the chromatin; each successive turn of the coil lies on top or anterior to the preceding turn, with the end ultimately extending from the anterior surface of the coil out into the false discharge. Thus, looking down on the coil we see on top the turn of the bundle that will start the false discharge; on the bottom we see the turn that cuts back to the middle and enters the nuclear canal. From the replicas we can easily see that the coil then is a right-handed helix. We examined 20 images similar to those illustrated in Fig. 9. All were right handed.

Changes in the Filament Bundle in Going from the Coil to the False Discharge: Computer Simulation of the Motion

In the reaction in which the false discharge is generated, the bundle changes from being supercoiled to the right by 60° per arm to being supercoiled to the left by 30° per arm, i.e. in the false discharge. Thus, there is a change of 90° per arm. The effect of such a change in superhelicity is to rotate one portion of the bundle relative to the others. Fig. 10*a* shows a schematic representation of seven filaments (rods) joined by crossbridges (sheets). The six outer filaments wind helically around the central one. As the superhelicity changes by 90°, features (e.g.

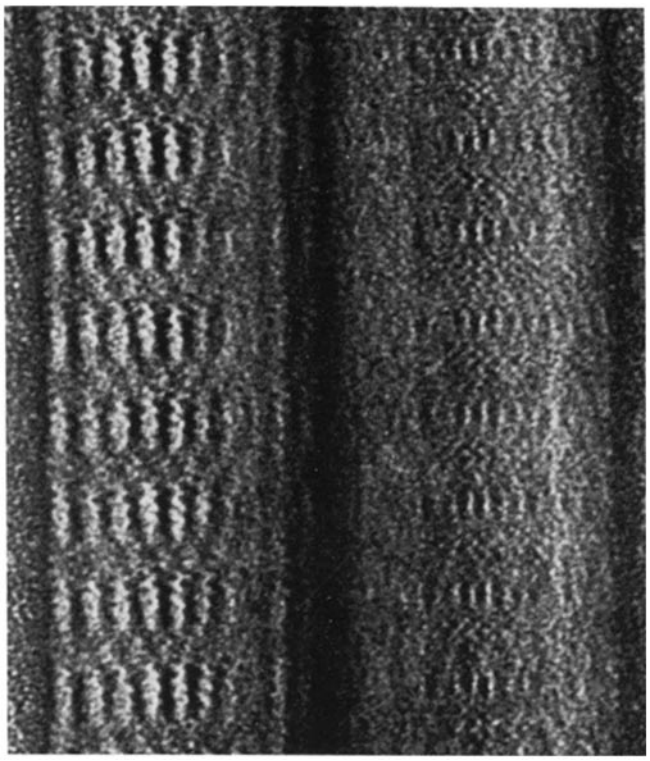

FIGURE 8 False discharge that has been converted to a true discharge. A preparation of false discharges is converted to a form that appears exactly like the true discharge. Note in the converted structure that the supercoiling and elbows are absent. × 325,000.

an elbow) indicated by the arrow rotate 90° relative to each other. The important point is that the elbows, which all lie in a common plane in the coil, when rotated by 90° relative to each other as a result of the 90° change in supercoiling (Fig. 10*b*) produce a structure that takes the form of a left-handed helix. Thus, if each successive arm changes its superhelicity by 90°, a left-handed helix will be generated which screws its way into the surrounding medium. One complete rotation of the process occurs every four arms (4 × 90° = 360°) and, if the length of the arms remains constant, then a repeat occurs every 2.8 μm (4 × 0.7 μm). Thus, the change in the superhelicity we measured accounts completely for the form and motion of the false discharge. We have simulated this using the computer. We divided the motion up into 300 frames. Between frames the most distal elbow is rotated by 3° relative to the plane of the coil. After 30 frames this elbow is rotated the required 90° and we move on to the penultimate elbow, and so on. In addition, between frames we also rotate the coil to feed the growing false discharge. When all this is put together, it mimics the false discharge seen in the movies. Compare this sequence (Fig. 11) with those of the movie in Fig. 3. Note how the tip in both undulates with the extension. The animation shows that we can account for the motion in detail.

DISCUSSION

The true discharge, the false discharge, and the coil are different states of the actin-filament bundle; each state is convertible to another except the true discharge which seems to be the "end state" of the bundle (see reference 1 and this paper). In our last paper (5) we described the motion of the filament bundle in going from the coil to the true discharge. We suggested that a change in twist of the actin filaments themselves generates the motion. In this paper we have concentrated on the false discharge and will show below that this motion also can be most easily accounted for by a change in twist of the actin filaments. In fact, the same helical form of the bundle found in the false discharge is generated during the true discharge but as a transient intermediate between the straight, true-discharge form and its precursor—the coil. Thus, the false discharge tells us more about how this bundle produces force. Before relating all these movements and their molecular mechanisms into one simple model, let us review the relevant facts:

(*a*) The bundle is polar; that is, if all the actin filaments in the bundle were decorated with the S1 subfragment of myosin, the arrowheads would uniformly point away from the acrosomal vesicle (11).

(*b*) The direction of motion of the bundle in the false discharge is opposite that in the true discharge. The motion of the false discharge is posteriorly and in the direction that actin would be moved by myosin. The motion of the bundle during the true discharge and during the retraction of the false discharge, however, is anteriorly and opposite to the direction that actin would be moved by myosin.

(*c*) The extension of the false discharge begins at the posterior end of the bundle. This is opposite that of the true discharge, which begins at the anterior end of the bundle.

(*d*) The bundle, in each of its three states, is a rigid structure which retains its form when freed from the cell (10).

(*e*) Change in the supercoiling of the bundle and in the twist of filaments accompanies the discharge.

Possible mechanisms for the extension can be divided into two classes: the first is one in which the bundle, a passive structure, is pulled or pushed by a myosinlike structure external to it; and in the second, changes within the bundle itself generate the force for extension. In our first paper (5), we rejected the first possibility because the direction of motion in the true discharge is opposite that expected for actomyosin, because the rigidity of the bundle is inconsistent with its role as a passive structure, and because we actually observe structural changes within the bundle which suggest an active role. Instead, we suggested in that paper that a change in twist of the filaments in the bundle drives the extension. We now show how this same mechanism also explains the false discharge.

Extension or Retraction of the False Discharge Can Be Explained by a Change in Pitch of the Actin Helix

We demonstrated that in going from the coil to the false discharge each arm changes its superhelicity which in turn results in a 90° rotation of the affected arm relative to its neighbor still remaining in the coil. The key question is what brings about this change in superhelicity and thus the rotation. What we are proposing is that a change in the twist of the filaments is the reaction that drives both the change in superhelicity and the extension. We demonstrated that the subunits within each filament of the false discharge are in a different position than those in each filament in the coil; that is, each subunit has moved 0.35° in going from the coil to the false discharge. It is this change in the intrafilament bonding then that will change the superhelicity of the filaments. In Fig. 10*a* we illustrate this point. The asterisk that denotes the position of a feature on the bundle (e.g. an elbow) equally can denote the position of a feature on a filament (e.g. an actin subunit).

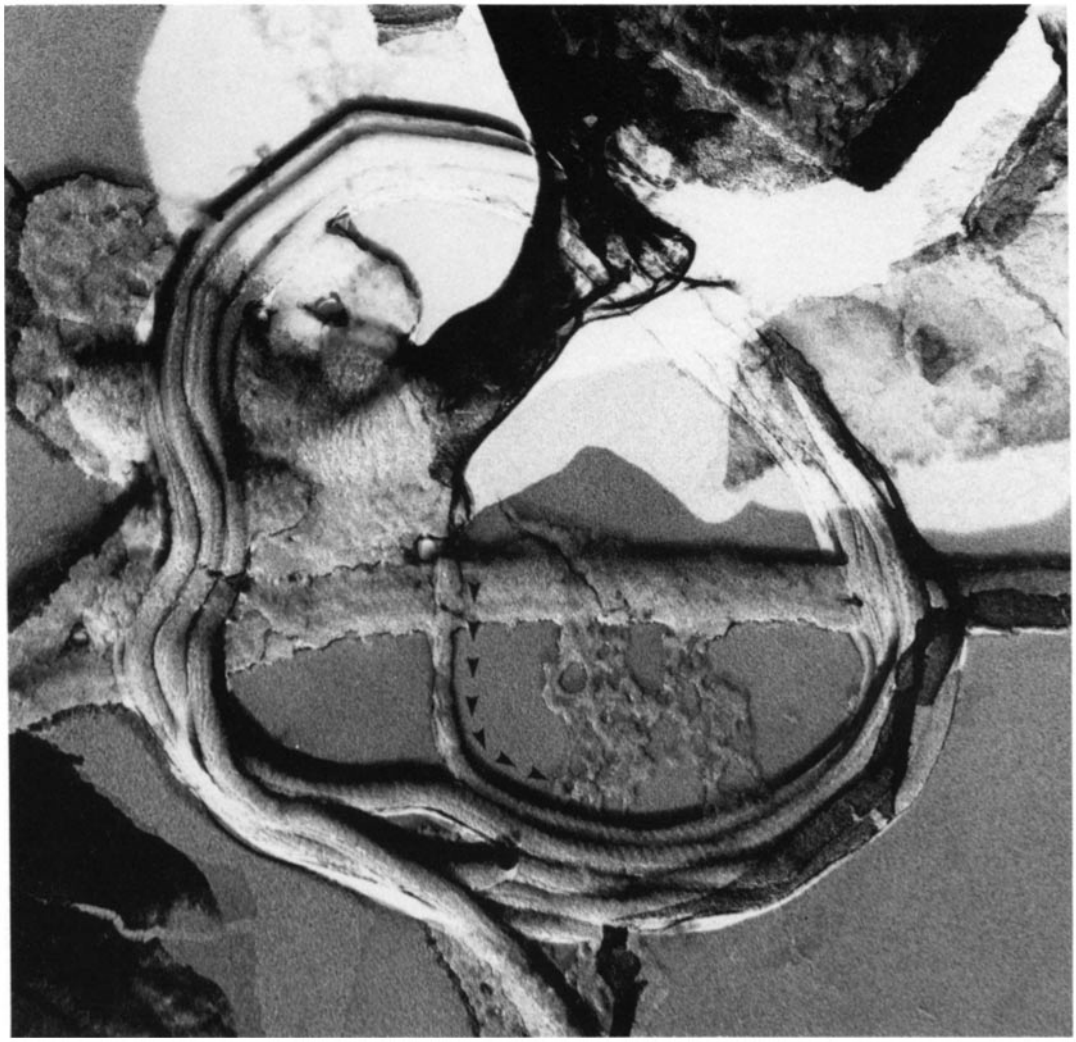

FIGURE 9 Electron micrograph of a shadowed coil. The micrograph clearly shows the hand of the coil. The segment of the bundle from the nuclear canal (see arrow) is vertical. When it reaches the coil it joins the counterclockwise turn of the coil nearest the grid (see arrow). This shows definitively that the coil is a shallow, right-handed helix. × 35,000.

Clearly, the angular position of a subunit at the top of the bundle rotates relative to that at the bottom by the same amount that the elbows rotate relative to each other. Although changes in pitch of the helix have little effect on the length of the filament, they lead to an uncoiling of the bundle. This process is analogous to movement in a spring in which changes in length of the spring are not due to changes in length of the wire that composes the spring but rather are due to an uncoiling of the spring. The elongation of a spring, then, is necessarily accompanied by and can be driven by torsional energy stored in the wire; thus, changes in the length of a compressed spring are accompanied by, and, more important, are driven by, changes in the twist of the wire comprising the spring.

Now let us put all the observations together and relate them to the extension of the false discharge as observed from our movies and from electron micrographs. The false discharge begins at the distal or thick end of the bundle. As the filaments change twist, the right-handed supercoiling is undone, resulting in rotation of the distal end of the bundle (Fig. 12). As the zone of untwisting moves from arm to arm, neighboring elbows rotate 90° or are moved from coplanar to perpendicular which generates a left-handed helical process having the observed repeat of 2.8 μm. Since the process generated by the false discharge often moves out along a fixed direction, the coil must be rotating in order to feed the bundle into the growing process. What is important is that the change in twist of the filaments and the uncoiling do not alter the elbows in either their positions or their angular bend in either the coil or the false discharge. Thus, the angle of bend is 156° in both cases and the separation between elbows is 0.7 μm in both cases. If the position of the elbow were moved significantly along the bundle during the false discharge, it would cause a noticeable movement away from the precise screwing motion observed in the light microscope. We presume that elbows are features locked into the structure by means of the interfilament cross bridges and that during changes in the twist of the filaments the interfilament cross bridges remain intact, maintaining the form and position of the elbow. We envision that the region corresponding to the elbow is differently cross-bridged than the region corresponding to the arm.

Extension of Both the False Discharge and True Discharge Can Be Explained by a Change in Twist of the Actin Helix, and are Related

Let us now examine the true discharge and compare its antics with those of the false discharge. The point of view we adopt is that both these structures and their movements are

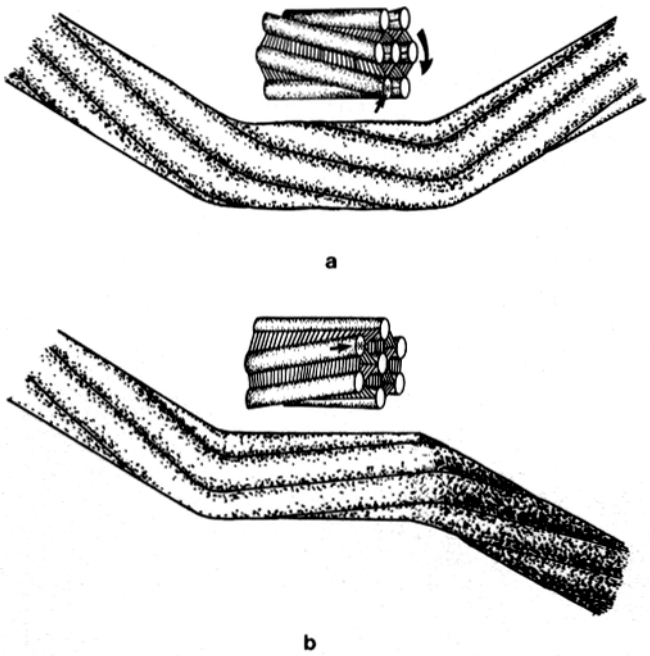

FIGURE 10 Effect of change in supercoiling. (*a*) Segment of three arms of the bundle in the coil. The right-hand segment has already undergone a change and is supercoiled in a left-handed sense. The central arm is still in the coiled state, that is, is supercoiled in a right-handed sense. The small figure above the central arm more clearly shows the filaments. (*b*) When the central arm changes its supercoiling by 90° as happens during the false discharge, the plane of the right elbow rotates 90°. This effect is more clearly seen in the small figure. Note that in changing supercoiling by 90° (i.e. in going from *a* to *b*) the right side of the bundle rotates by 90° with respect to the left-hand side. In the bundle, the effect is to rotate the plane of the right elbow with respect to the left elbow. In *b* the plane of the left arm is perpendicular to the plane of the drawing. Here, the amount of rotation has been exaggerated.

related. Let us begin by summarizing their similarities. In both, the filaments, in going from the coil to the discharge, albeit false or true, undergo a change in twist (they untwist), and in both this results in a change in superhelicity. Both structures rotate as they discharge and in both each rotation is coupled to translation (elongation). Furthermore, segments of a false dischargelike helix are present in the form of kinks in the true discharge. Moreover, in vitro the false discharge can transform in part or entirely into a true discharge. The differences between the true and false discharge are first that the true discharge develops from opposite ends of the same bundle and secondly that in generating the true discharge not only must there be a change in twist, but, unlike the formation of the false discharge, there also has to be a melting out of the elbows. The melting of elbows is not essential since kinks often appear in the true discharge; these kinks consist of four arms and four elbows and are, in fact, segments of the false discharge form that have not melted out their elbows. Thus, the false discharge form is an intermediate between the true discharge and the coil. The interesting and important feature here is that, for the formation of both false and true discharges, which are intimately connected, the same mechanism seems to be responsible, namely an active change in pitch of the filaments.

How Might the Change in Twist of Actin Be Achieved

A change in twist must correspond to a shift in the intersubunit bonds within a filament. This type of shift in structure as a result of a change in intersubunit bonds is best typified by hemoglobin (7). In moving from high oxygen tension to low oxygen tension, the subunits in the tetrameric structure move relative to one another, i.e. from the oxy form to the deoxy form. When the oxygen tension is again raised, they return to the oxy form. Thus, cyclic changes in the oxygen tension cause cyclic changes in hemoglobin structure.

The point of the analogy is to suggest that the interaction between monomeric units in a filament can undergo such cyclic changes. In this case the change in the intrafilament bonds between subunits leads to a change in the twist of the filament.

Although we do not know what substance causes a change in intersubunit interactions in *Limulus*, we think it reasonable to expect that the trigger for a change in intersubunit interactions might be a change in concentration of small molecules or a combination of small molecules. For example, we know that *Limulus* sperm can be induced to undergo the acrosomal reaction by the addition of ionophores to the sea water surrounding the sperm. Excess calcium will also induce the reaction. Yet actin is not the only molecule in these bundles: there are two others—a 55,000-mol wt protein and a 95,000-mol wt protein. We suspect that these proteins may be important together with actin in inducing a change in twist of the actin helix. Our supposition comes from the studies of Egelman and DeRosier (unpublished observations) who showed that in Mg^{++} paracrystals (and in isolated filaments) of sea urchin actin the angle between successive subunits in the helix is 166.15° whereas in bundles made by combining actin filaments and fascin a 55,000-mol wt protein isolated from sea urchin eggs the angle is 166.67°. Thus, there is a difference in twist of

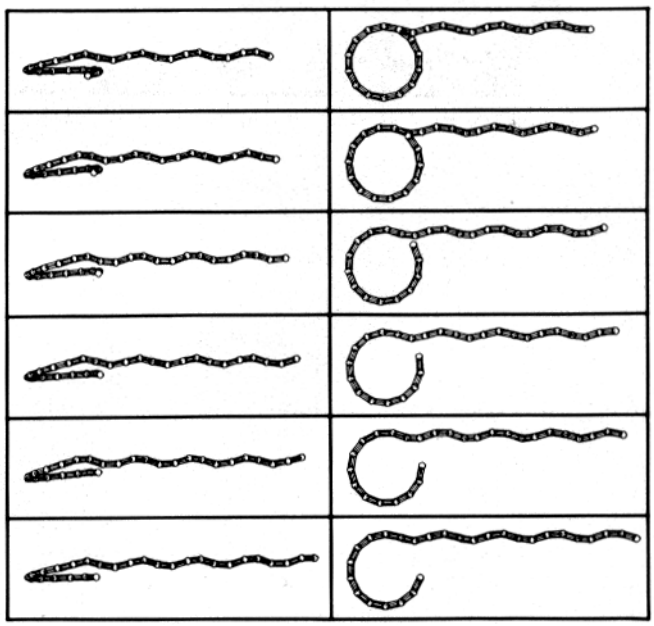

FIGURE 11 Frames from a computer movie of the false discharge. The relative motion of the elbows during the false discharge is easily animated. The change in supercoiling has the effect of rotating the elbows by 90°. The rotation was divided into 30 three-degree steps. At each succeeding step, the whole segment of the bundle on the right is rotated three degrees and the coil rotated 24/30 = 0.8° to feed the growing false discharge. Six frames were chosen which approximate those in Fig. 3. The effect mimics the movies of the false discharge. Note that the advancing tip of the bundle begins on a crest, falls to a trough, and again climbs to a crest, exactly as seen in the movie.

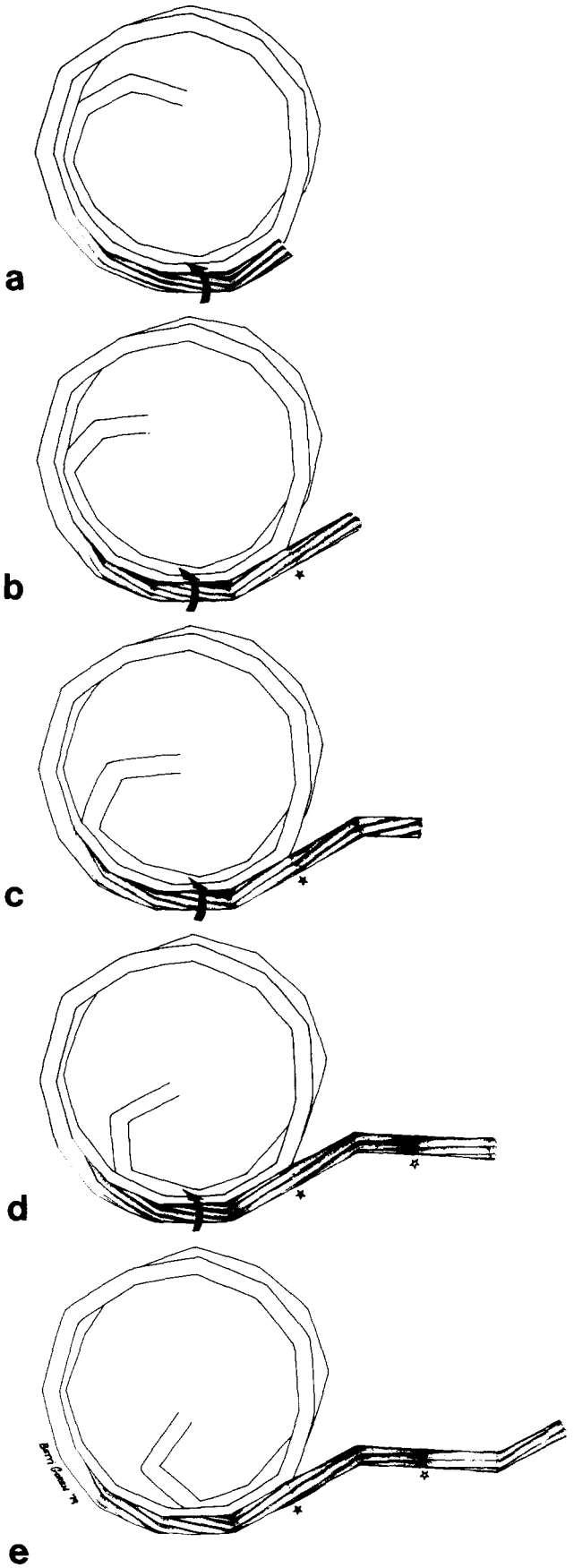

FIGURE 12 Sequence depicting the generation of the false discharge. The reaction begins with a change in the supercoiling of the penultimate arm (see arrow in *a*) and is accompanied by a rotation of 1/14th of a revolution which feeds the growing false discharge. The change in supercoiling is 90° per arm and causes the last elbow to rotate 90° so that it points convex side up and the turning of the coil places arm 3 where arm 2 was. In frames (*b*) to (*e*) the process in (*a*) repeats. In (*e*), one repeat of the false discharge has been generated. The repeat consists of four arms. The filled stars indicate elbows that are convex side up. The unfilled stars indicate elbows that are concave side up.

0.52° per subunit. Thus the molecules that bind adjacent actin filaments into a bundle can affect the twist of filaments that make up the bundle. Ions, then, by affecting conformation of component macromolecules could induce a change in twist of the actin filaments.

CONCLUSIONS

(*a*) We propose that the discharge, whether false or true, is driven by forces generated within the component filaments. The forces from the individual filaments are mechanically coupled by the cross-bridges between filaments so that, if there are 50 filaments, the force driving the extension is 50 times that due to one filament.

(*b*) The force results in a shift of the intrafilament bonds corresponding to a change in twist of each component filament.

(*c*) The change in twist of each filament concomitantly changes the supercoiling of filaments in the coiled bundle.

(*d*) The change in supercoiling causes rotation of the elbows relative to each other and changes the bundle from a flat, compact right-handed helical coil to a left-handed, extended structure.

(*e*) In the false discharge, the distal end is unconstrained and extends out laterally from the plane of the coil as predicted by the computer model. It is a reversible reaction so that upon restoration of the initial intrafilament bond the false discharge will retract back to the coil form.

(*f*) In the true discharge, the apical end is constrained by the nuclear canal which directs the extension anteriorly. Unlike the false discharge, during the true discharge the elbows are "melted out." This second step is not essential to the extension since occasionally elbows are found in the true discharge. The importance of this second step in which the elbows are "melted out" is that it makes the extension irreversible. Thus, even if the filaments revert to their original state of twist in the coil, without the elbows the coil cannot reform.

Generality of our Observations on Limulus Sperm to Other Systems

In contrast to muscle contraction in which force is generated by cyclic interactions between two types of filaments, actin and myosin, we propose that motion in the *Limulus* bundle results from a change in the internal bonding of the subunits that make up the filaments. Thus, in *Limulus* sperm the bundle drives itself. All that is required is that the intrasubunit bonding within each filament produce a change in the twist of the filaments. The rest of the extension and retraction then follows.

This mechanism provides a view of a new dynamic property of actin-containing filaments, i.e. that of generating motion by a change of twist. The consequences of the change in twist depend on the mechanical construction of the bundle. Thus, in the coil of the sperm, this leads to a transition from a compact structure (the coil) to an extended one (the false or true discharge). In other systems the consequences might be quite different. Particularly striking in this regard is that the microvilli of the brush border and the microvilli on the surface of

sea urchin oocytes appear to be superhelical bundles of actin filaments (2, 9). Changes in the superhelicity driven by changes in the twist of filaments may be a dynamic property of such structures.

We want to thank Betti Goren and Adrienne Weinberger for the drawings, and Dr. Jim Fillers for his help in modifying and using a model building computer program. We also thank Penny Caponigro and Louise Seidel for their help with the manuscript. We acknowledge the kindness of Dr. John Heuser in whose laboratory some of the freeze-etched images were prepared while one of us (L. G. Tilney) was on sabbatical.

This research was supported by grants from the National Institutes of Health grant GM26357 (to D. J. DeRosier) and HD14474 (to L. G. Tilney).

Received for publication 11 August 1981, and in revised form 5 January 1982.

REFERENCES

1. André, J. 1965. A propos d'une leçon sur la Limule. *Ann. Fac. Sci. Clermont.* 26:27–38.
2. Begg, D. A., R. Rodewald, and L. I. Rebhun. 1978. The visualization of actin filament polarity in thin sections. *J. Cell Biol.* 79:846–852.
3. DeRosier, D. J., E. Mandelkow, A. Silliman, L. G. Tilney, and R. Kane. 1977. The structure of actin-containing filaments from two types of non-muscle cells. *J. Mol. Biol.* 113:679–695.
4. DeRosier, D. J., and P. B. Moore. 1970. Reconstruction of three dimensional images from electron micrographs of structures with helical symmetry. *J. Mol. Biol.* 52:355–369.
5. DeRosier, D. J., L. G. Tilney, and P. F. Flicker. 1980. A change in the twist of the actin containing filaments occurs during the extension of the acrosomal process in *Limulus* sperm. *J. Mol. Biol.* 137:375–389.
6. Heuser, J. E., and M. W. Kirschner. 1980. Filament organization revealed in platinum replicas of freeze-dried cytoskeletons. *J. Cell Biol.* 86:212–234.
7. Perutz, M. F. 1978. Hemoglobin structure and respiratory transport. *Sci. Am.* 92–125.
8. Salmon, E. D., and D. J. DeRosier. 1981. A surveying optical diffractometer. *J. Micros. (Oxf.).* 123:239–247.
9. Spudich, J. A., and L. A. Amos. 1979. Structure of actin filament bundles from microvilli of sea urchin eggs. *J. Mol. Biol.* 129:319–331.
10. Tilney, L. G. 1975. Actin filaments in the acrosomal reaction of *Limulus* sperm. *J. Cell Biol.* 64:289–310.
11. Tilney, L. G., E. M. Bonder, and D. J. DeRosier. 1981. Actin filaments elongate from their membrane-associated ends. *J. Cell Biol.* 90:485–494.